



Article

# An Experimental Study Incorporating Carbon Fiber Composite Bars and Wraps for Concrete Performance and Failure Insight

Ali Akbarpour , Jeffery Volz and Shreya Vemuganti \*

School of Civil Engineering and Environmental Science, University of Oklahoma, 202 W. Boyd St., Room 334, Norman, OK 73019, USA; ali.akbarpour@ou.edu (A.A.); volz@ou.edu (J.V.)

\* Correspondence: svemugan@ou.edu

**Abstract:** Corrosion of conventional steel reinforcement is responsible for numerous structurally deficient bridges, which is a multi-billion-dollar challenge that creates a vicious cycle of maintenance, repair, and replacement of infrastructure. Repair of existing structures with fiber-reinforced polymer (FRP) has become widespread due to multiple advantages. Carbon FRP's superior tensile strength and stiffness make it particularly effective in shear and flexural strengthening of reinforced concrete (RC) beams. This experimental study incorporates carbon fiber polymer composite bars and wraps to study and report on the flexural behavior of RC beams. By employing a combination of CFRP bar and wrap for strengthening RC beams, this study observed an approximate 95% improvement in flexural load capacity relative to control RC beams without strengthening. This substantial enhancement highlights the effectiveness of integrating CFRP in structural applications. Nevertheless, the key observation is the failure mode due to this combination providing significant insights into the changes facilitated by this combination approach.

**Keywords:** near-surface mounting (NSM); U-wrap; fiber-reinforced polymer (FRP); carbon fiber-reinforced polymer (CFRP); strengthening; reinforced concrete



**Citation:** Akbarpour, A.; Volz, J.; Vemuganti, S. An Experimental Study Incorporating Carbon Fiber Composite Bars and Wraps for Concrete Performance and Failure Insight. *J. Compos. Sci.* **2024**, *8*, 174. <https://doi.org/10.3390/jcs8050174>

Academic Editor: Jiadeng Zhu

Received: 29 March 2024

Revised: 30 April 2024

Accepted: 7 May 2024

Published: 9 May 2024



**Copyright:** © 2024 by the authors. Licensee MDPI, Basel, Switzerland. This article is an open access article distributed under the terms and conditions of the Creative Commons Attribution (CC BY) license (<https://creativecommons.org/licenses/by/4.0/>).

## 1. Introduction

The American Society of Civil Engineers (ASCE) 2021 report card for infrastructure scored a C-, which indicates a mediocre condition with signs of deterioration and deficiencies in condition and functionality. Reinforced and prestressed concrete infrastructure built in the 60s and 70s is now observing severe deterioration, and action is needed to ensure the structural performance is adequate for the demands imposed. Infrastructure from the 60s–70s is now reaching the end of its service life, with marked deterioration becoming increasingly evident. Quantitative studies reveal that up to 60% of bridges constructed in temperate climates during this era exhibit significant structural decline, primarily due to corrosion of steel reinforcement, with most showing severe deterioration after surpassing the 50 year mark. This widespread degradation underlines the urgency for rehabilitation methods that can extend the lifespan of these critical structures [1]. Corrosion of conventional steel reinforcement is responsible for numerous structurally deficient bridges, which is a multi-billion-dollar challenge that creates a vicious cycle of maintenance, repair, and replacement of infrastructure. This presents a higher risk for future closure or weight restrictions and requires substantial investment. Repair and strengthening techniques can provide a cost-effective means to extend the service lives of bridges efficiently and safely. This is necessary to accommodate rising traffic volumes and to comply with contemporary design standards [2,3].

In recent years, fiber-reinforced polymers (FRPs) have garnered considerable interest from the engineering community, resulting in the widespread adoption of composite structures by the construction industry [4]. FRPs have been adopted for the repair and strengthening of infrastructure. Its usage spans a range of geographic regions from the

harsh climates of Northern Europe and North America to the tropical environments of Southeast Asia, illustrating its versatility and reliability in diverse conditions. Economically, despite higher initial costs compared to traditional materials, FRP offers significant long-term benefits through reduced maintenance and repair costs, supporting its cost-effectiveness and extensive use in both developed and developing economies [5]. The progress in FRP composites, particularly in aerospace applications, has underscored their potential for civil engineering uses [6]. FRP's resistance to corrosion contributes significantly to enhancing strength and durability in various applications [7]. FRP's corrosion-resistant properties are critical in its role in prolonging the structural integrity of retrofitted steel columns, making it an invaluable material in the rehabilitation of aging infrastructure plagued by corrosion-related deterioration [8]. FRP is composed of a polymer matrix with different types of fibers. The specific type of FRP is defined based on the kind of fiber employed [5]. Diverse fibers such as glass, carbon, aramid, and basalt are utilized in FRP due to their high strength, stiffness, and low-density characteristics [9]. In the field of construction, carbon-fiber-reinforced polymers (CFRP) and glass-fiber-reinforced polymers (GFRP) are widely used due to their robust properties [10,11]. Yet their application is limited in environments requiring high fire resistance standards due to the vulnerability of CFRP composites to degradation at elevated temperatures. Compared to steel, CFRP can offer five times the strength of steel. Although CFRP's initial costs are higher than those of steel, its maintenance-free properties and lighter weight provide significant long-term economic and structural benefits, making it a valuable alternative depending on project-specific demands. CFRP and GFRP are both used for structural strengthening but differ significantly in their mechanical properties. CFRP exhibits tensile strengths of 3500 to 6000 MPa and an elastic modulus of 230,000 to 250,000 MPa, making it ideal for high-stress applications. In contrast, GFRP has tensile strengths of 1500 to 2500 MPa and an elastic modulus of 70,000 to 90,000 MPa [12]. This enables CFRP to be more effective in reducing deformations in reinforced concrete (RC) structures [13]. CFRP's superior tensile strength and stiffness make it particularly effective in shear and flexural strengthening of RC beams, offering improved ability of RC beams to resist mechanical stresses and maintain structural integrity under increased loads [14].

In flexural strengthening of RC beams with the usage of FRP, two approaches are suggested by the American Concrete Institute (ACI) 440-2R [15]: near-surface-mounted (NSM) FRP and externally bonded (EB) FRP [16,17]. EB-FRP involves attaching an FRP laminate to the beam's tension side using epoxy, allowing the laminate to serve as extra reinforcement and boost the beam's flexural strength [16]. NSM-FRP entails creating a groove on the beam's tension side, partially filling it with epoxy, inserting an FRP bar or strips, and then completely sealing it with epoxy [17]. The primary benefit of the NSM-FRP method is its bonding efficiency with the concrete [18]. The bonding efficacy is crucial for NSM-FRP's performance, as demonstrated in Figure 1.

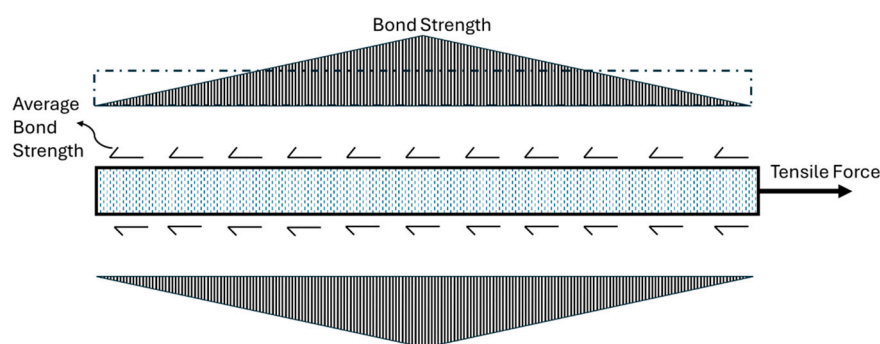


**Figure 1.** Transfer of forces in a NSM FRP bar (developed from ACI 440-2R).

For flexural strengthening using NSM-FRP for RC beams, CFRP is often preferred over GFRP. CFRP is often the material of choice due to its superior axial stiffness and tensile

strength [19]. This allows for a reduction in the necessary concrete cover area for NSM-FRP, optimizing the use of space and materials in construction projects [20]. The failure modes for RC beams incorporating the NSM-FRP technique typically include FRP rupture or debonding post tension steel yield [21]. Research by Hassan and Rizkalla [5] suggests that FRP rupture is unlikely in NSM-FRP with an adequate length of NSM-FRP bars. This is because the FRP bar generally only reaches about 60–70% of its maximum tensile capacity, indicating a lower risk of rupture under normal conditions. Therefore, in the context of NSM-FRP-strengthened RC beams, debonding is often the primary mode of failure. Often, U-wrap shear strengthening is performed on RC beams in combination with NSM flexural strengthening to meet both demands. The U-wrapping method, utilizing wet layup, involves saturating FRP fabric in epoxy and adhering it to concrete surfaces in the direction of shear reinforcement [22]. This method has been implemented in various configurations, including complete U-wraps, three-sided U-wraps, and two-sided U-wraps [23]. Extensive research has examined the impact of different wrapping schemes on the efficiency of shear strengthening in beams and columns [24–26]. The application of externally bonded systems employing an inorganic matrix, such as fabric-reinforced cementitious matrix (FRCM) composites, has been recognized for its enhanced thermal resistance and structural integrity in elevated temperature environments [27]. Studies have shown that combining U-wrap FRP with NSM steel significantly enhances flexural load capacity, effectively preventing premature failures in RC beams reinforced solely with NSM steel [28].

The primary focus of this study was to comprehensively evaluate the flexural response of 20 laboratory scale RC beams strengthened with NSM-CFRP and U-wrap CFRP individually and as a combination. The load displacement behaviors of each beam were carefully recorded in addition to data from strain gauges at multiple locations in the beam. Visual inspection of failure modes was performed. Emphasis was also placed on optimizing surface preparation techniques for both methods to enhance the efficacy of the strengthening systems. The findings aim to provide insightful recommendations for the application of CFRP systems for strengthening RC beams, potentially informing future updates to design codes and engineering practices.

## 2. Materials and Methods

### 2.1. Materials

This study utilized 20 RC beams divided into five groups to evaluate the impact of different FRP strengthening systems: control group ('C'), U-wrap group ('U'), NSM group ('N'), NSM and U-wrap group ('NU') and NSM and shear zone U-wrap group ('NSU'). C beams were used to establish a baseline performance. To isolate the effects of U-wrap and NSM, U and NU groups were used. For the combination of NSM and U-wrap, full U-wrap and shear zone U-wrap were considered to obtain two types of confinement effects.

The concrete employed featured a maximum nominal aggregate size of 12.7 mm, with an observed slump measuring  $10 \pm 1.2$  cm. The slump test was performed using the ASTM C143 [29]. The chosen maximum nominal aggregate size of 12.7 mm improves the concrete mix by enhancing workability, reducing shrinkage, and optimizing mechanical strength. Larger aggregates help achieve a better void ratio, decrease cement paste use, and consequently enhance the structural and economic efficiency of the concrete. To assess the mechanical characteristics of the selected mix design, three distinct experimental tests were conducted. The unconfined compression tests were carried out in accordance with ASTM C39 [30] on samples after 7 and 28 days of curing. Furthermore, for a comparative analysis, the compressive strength of samples subjected to heat curing was evaluated at the age of 7 days. Also, the split tensile strength of specimens was evaluated at the age of 28 days based on ASTM C496 [31]. Moreover, the elastic modulus of the specimens was assessed following the ASTM 469 [32]. At 28 days, the average compressive strength of the concrete was 53.09 MPa with a standard deviation of 1.78 MPa. The split tensile strength recorded was 3.49 MPa with a standard deviation of 0.16 MPa. Additionally, the elastic modulus was determined to be 27,636 MPa. Each test result is a mean value of three tested specimens.

No. 3 (10 mm) NSM bars were acquired from RenewWrap®, as shown in Figure 2. The NSM strengthening systems involved using a specialized 2 part epoxy resin NSM gel, produced by the RenewWrap®. The guaranteed tensile strength provided by the manufacturer was 2171.85 MPa, and the tensile modulus of elasticity was 124.11 GPa with 1.75% ultimate strain. The U-wrap strengthening system technique was carried out using a unidirectional CFRP fabric, which was 1 mm thick, applied via a wet-layup method. Both the epoxy and the CFRP fabric used in this method were supplied by FyfeFRP, LLC. Specifically, unidirectional carbon fabric with the Tyfo S-330 epoxy was used in this study, as shown in Figure 2a. After 3 days of curing, the epoxy material properties as listed by the manufacturer had a tensile strength of 72.39 MPa, a tensile modulus of 3178 MPa, elongation of 5% and a minimum adhesion strength to concrete of 2.76 MPa. The composite's gross laminate properties as provided by the manufacturer included an ultimate tensile strength of 965.27 MPa, a tensile modulus of 93.08 GPa and elongation at break of 1%.

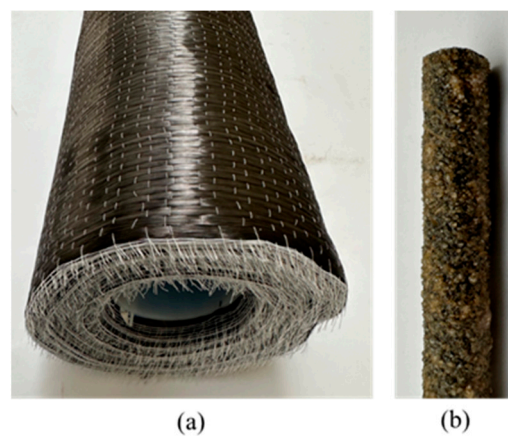


**Figure 2.** (a) Tyfo unidirectional CFRP fabric (b) No. 3 RenewWrap CFRP bar.

## 2.2. Methods

The beam groups were subjected to a displacement controlled static four-point bending test (2 loading points and 2 supports) until failure at a rate of 1 mm/min. The test was conducted using an MTS 810 with a 55 kip load cell and a data acquisition system. The load cell captured the resistance from the beams and machine displacement was recorded. Failure was defined when the load was reduced to more than 30% of the peak load. The loading points were spaced 152.4 mm apart and 660.4 mm between supports. In this study, flexural load capacity reported is defined as the maximum load a beam can support before failure when subjected to bending. The beams had a square cross-section, each with a depth of 152.4 mm. The beams were reinforced with four No. 3 (10 mm diameter) steel bars. Within these, two bars were allocated for compression reinforcement while the remaining two were used for tension reinforcement. The top cover was maintained at 29.5 mm and the bottom cover at 25.4 mm. This configuration was integral to the structural setup of each beam. For shear reinforcement, No. 3 stirrups, also 10 mm in nominal diameter, were spaced at intervals of 76 mm. After the concrete beams were cast, they were placed in heat curing for 7 days.

To facilitate strain readings, strain gauges were attached in four locations: concrete compression surface, steel compression surface, steel tension surface, and CFRP bar surface. To ensure the strain gauges were well attached, steps were adopted sequentially (1). Surface preparation: Initially, the surface underwent grinding using various grinders, selected based on the material. Subsequently, the surface was thoroughly cleaned, rendering it prepared for the subsequent steps. (2). Surface cleaning: to eliminate any dust and oily residues from the specimens' surfaces, a combination of three cleaning agents—acetone, a water-based acidic surface cleaner, and a water-based alkaline surface cleaner—was employed. (3). Strain gauge attachment: following the meticulous cleaning and preparation

of the material surfaces, strain gauges were affixed using either super glue or epoxy. (4). Surface finishing: To safeguard the strain gauges during the concrete casting process and subsequent phases, a protective surface finishing was implemented. Super 88 Scotch tape was applied to shield the wires, Silicone RTV adhesive sealant was utilized to guard against water exposure, and Nashua 367-17 foil mastic sealant was employed for protection against aggregates. Figure 3 shows the strain gauges attached to different materials.

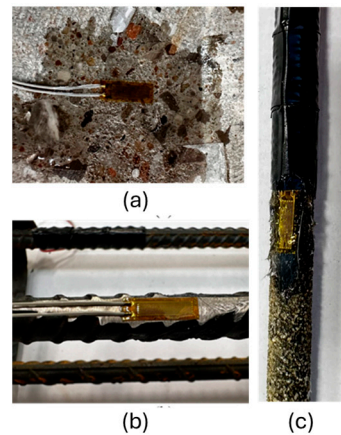


**Figure 3.** Strain gauge on (a) on concrete (b) steel (c) NSM CFRP.

#### 2.2.1. U-Wrap Shear Strengthening (U Type)

Three side U-wrapping is a technique employed for shear strengthening of concrete beams. Beams U, NU and NSU were strengthened using this CFRP wrapping technique. The concrete surface was prepared to a minimum concrete surface profile as defined by the CFRP fabric manufacturer's guidelines, ACI 440-2R and ICRI surface profile. Abrasive grinding was performed on flat concrete surfaces and for wrapping around edges using a 1.2 cm radius rounded grinder. The prepared surface was cleaned using a water jet and compressed air. The beams were allowed to air dry for twenty-four hours to remove moisture on the surface of the beams. Surface preparation is shown in Figure 4.

Part A and Part B mixed resin was initially applied as a prime coat on the concrete surface using a soft roller. Mix ratio of Tyfo S-330 according to the manufacturer was 100A:34.5B by weight. For U and NU beams, the CFRP fabric was cut to specified dimensions: 406 mm along the two sides and the bottom of the beam in the direction of the fibers, and a length of 660 mm opposite to the fiber direction, equal to the length between the two supports for the beam. For the NSU beams, the U-wrap was only applied in the shear area. After cutting the fabric, the CFRP fabric was saturated in epoxy. Saturated fabric was wrapped around the beam and a hard roller was employed to eliminate any trapped air and ensure even layup as illustrated in the figures below. Wrapped beams were allowed to cure for 14 days at room temperature to enable complete hardening of the wrapping and have composite action with the beams. Figures 4–7 show the steps of U-wrapping technique.

#### 2.2.2. NSM Flexural Strengthening (N Type)

In the beam series labeled 'N', 'NU', and 'NSU', which underwent NSM-CFRP flexural reinforcement, each was constructed with an integrated groove on the tension face. To facilitate the creation of the groove on the tension side of the beam, a plastic piece, measuring 25.4 mm in width and depth, was affixed to the concrete form using a double-sided adhesive tape. Twenty-four hours after casting, specimens were demolded and the plastic piece was removed, and they were subjected to heat curing for a period of 7 days. Following a 7 day heat curing process, the surface underwent a grinding process using a wire brush, followed by cleaning with a water jet, as shown in Figure 8. The prepared surface was then left to air dry for a day to eliminate any lingering moisture from the surface of the groove. To ensure the NSM groove was devoid of dust and unwanted materials, compressed air was used to remove any remaining particles. These meticulous steps were taken to guarantee

the cleanliness of the NSM groove, free from dust, moisture, and unwanted substances. Special attention was given to surface preparation to achieve a rough surface, ensuring a strong mechanical bond between the NSM gel and the concrete, thereby preventing any potential failure between the two materials.



**Figure 4.** Surface preparation for U-wrap to ensure adequate bond through surface and edge grinding. Part A and Part B mixing for prime coat application on beam prior to U-wrap.



**Figure 5.** (a) Carbon fiber fabric wetting process for U-wrap. (b) Rolling wet fabric onto plastic pipe for layup on beam.



**Figure 6.** Rolling wet fabric onto pre-marked beam covering three sides for U-wrap.

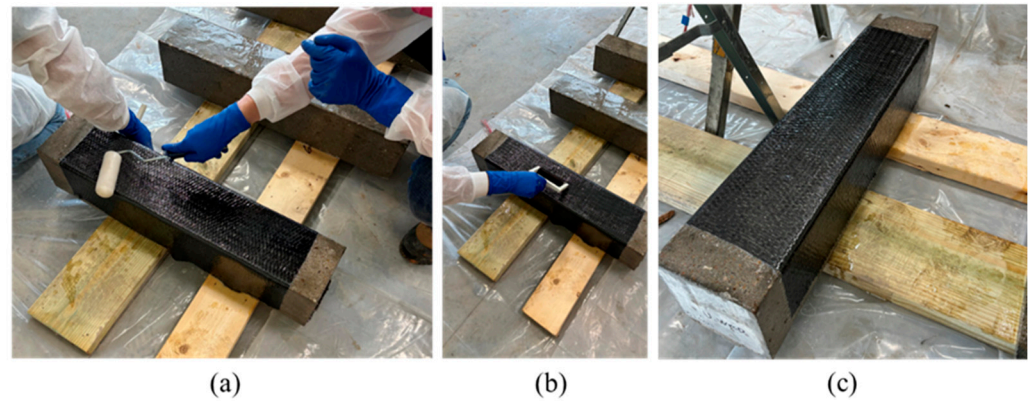


**Figure 7.** Wet layup process (a). Layup with soft roller (b). Layup with hard roller (c). Finished beam after U-wrap.

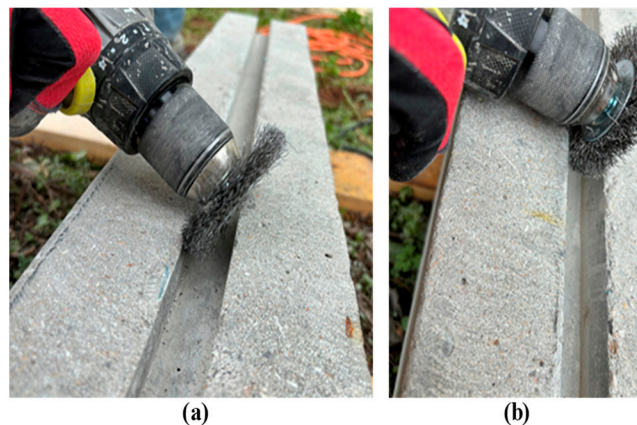


**Figure 8.** Grinding process for the NSM groove to ensure adequate bond between resin and concrete. (a) Use of wire brush for grinding inside the groove. (b) Closer look at grind surface.

NSM-CFRP flexural strengthening was performed utilizing carbon CFRP No. 3 bars with a nominal diameter of 10 mm and NSM gel. Figure 9 illustrates the different steps of flexural strengthening of the beams using the NSM-CFRP technique.

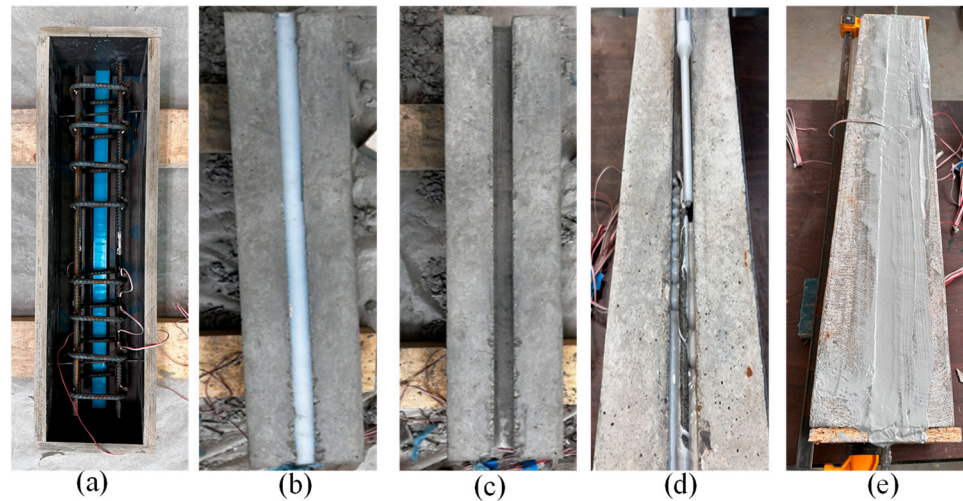


**Figure 9.** Steps of NSM-CFRP strengthening: (a) plastic form used at the bottom of the beam to create groove before casting, (b) beam after fabrication and hardening, (c) beam after removing plastic form, (d) dispensing NSM gel in the groove, (e) beam after performing surface preparation and NSM-CFRP flexural strengthening.

### 2.2.3. Combination of Shear and Flexural Strengthening Methods (NU and NSU Type)

NSM-strengthened beams for NU and NSU types were allowed to cure for 3 days for hardening of epoxy gel. The process described for U-wrap was adopted for the NSM-strengthened beams for NU and NSU types. Wrapped beams were allowed to cure for 14 days at room temperature to enable complete hardening of wrapping and composite action with the beams. Therefore, combination beams were cured after strengthening for a total of 17 days before testing. Figures 10 and 11 show the process of U-wrapping for NU and NSU beams.

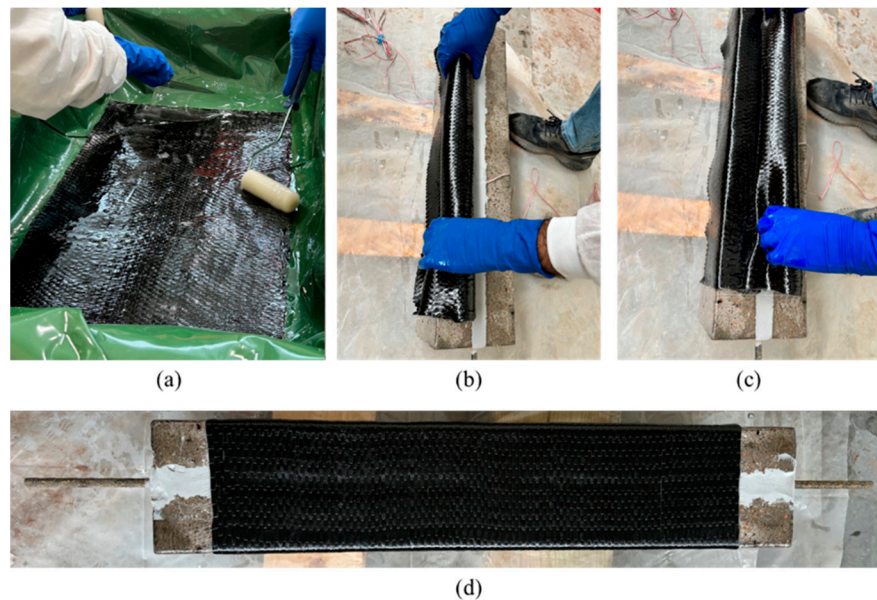


**Figure 10.** Combination strengthening NSM + complete U-wrap. (a) Wetting process of carbon fiber fabric, (b,c) wet-layup on NSM strengthened beams, (d) completed U-wrap strengthening on NSM-strengthened beam.

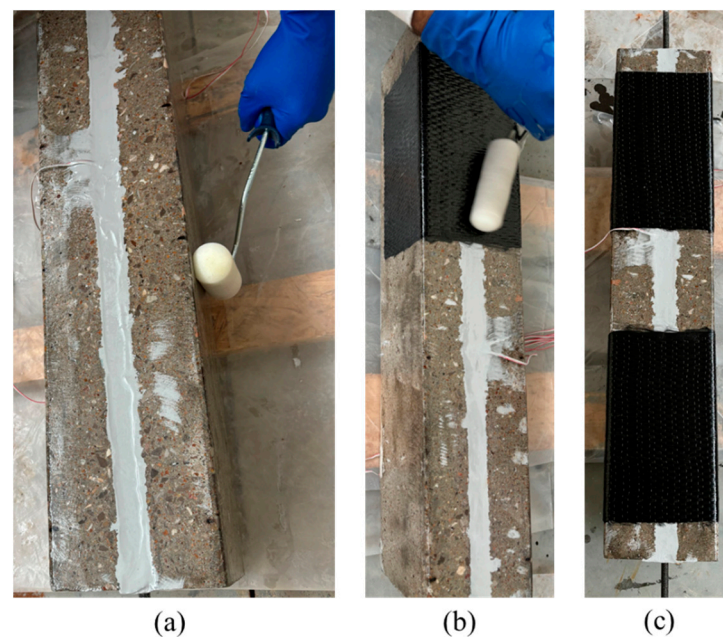


**Figure 11.** Combination strengthening NSM + shear only U-wrap (a) prime coat on NSM-strengthened beams for wet layup, (b) wet layup in shear only zones, (c) finished wet layup for U-wrap strengthening in shear-only zones for NSM-strengthened beams.

### 3. Results and Discussion

The comprehensive experimental findings for all types of the beams are systematically detailed in Table 1. The load–deflection data for a representative beam from each group is depicted in Figure 12. For the control group of RC beams, labeled C1 to C4, the average peak load at failure was found to be 79.19 kN, with a standard deviation of 2.99 kN. The mean deflection associated with this load was 8.70 mm, with a standard deviation of 8.70 mm. The load–deflection pattern of these beams exhibited typical RC beam characteristics, with linear elastic behavior observed up to approximately 50.5 kN, beyond which nonlinear behavior was noted up to the point of failure. For RC beams U1 to U4, reinforced with a CFRP U-wrap, the average peak load at failure was recorded as 94.42 kN, with a standard deviation of 7.19. The mean deflection measured for these beams was 9.73 mm, with a variation of  $\pm 0.84$  mm. The “U” series beams showed a conventional RC beam load–deflection profile, exhibiting linear elasticity up to an average load of 57.1 kN, after which nonlinear behavior was demonstrated up to the failure load. The RC beams N1 to N4, reinforced with NSM-FRP, showed an average ultimate load at failure of 144.60 kN, with a standard deviation of 18.39 kN. The corresponding average deflection was 9.60 mm, with a variation of  $\pm 0.91$  mm. The load–deflection characteristics of these “N” series beams differed notably from both the control “C” beams and the “U” series beams. In the “N” series beams reinforced with NSM-FRP, the load–deflection diagram exhibits linear elasticity up to an average load of 110 kN. Beyond this point, a slope change is noted, maintaining relatively linear behavior up to the maximum load. Nonlinearity then becomes obvious, and the load gradually decreases as the CFRP begins to slip, continuing until failure occurs. The RC beams designated as NU1 to NU4, which were reinforced with both NSM-FRP bars and U-wrap shear strengthening along their entire span, exhibited an average peak load at failure of 157.95 kN, with a standard deviation of 4.57 kN. The average deflection for these beams was measured at 12.86 mm, with a variation of  $\pm 2.01$  mm. Their load–deflection behavior maintains a linear behavior up the peak load. Beyond the linear elastic portion, NU-type beams demonstrated a slight change in slope in the load displacement behavior but continued to be linear until the first load drop, demonstrating a bilinear behavior.

**Table 1.** Load and deflection results upon test completion.

Beam Type	Load (kN)	Deflection (mm)	Failure Mode	Increase (%)
Control	79.19 ± 2.99	8.70 ± 0.46	CC	
U-wrap only	94.42 ± 7.19	9.73 ± 0.84	CC	19
NSM only	144.60 ± 18.39	9.60 ± 0.91	DB	83
NSM + U-wrap	157.95 ± 4.57	12.86 ± 2.01	R	99
NSM + shear U-wrap	162.17 ± 6.65	14.28 ± 2.23	R/SE	105

Notes: SE is splitting of epoxy cover, R is strength rupture of CFRP bar, DB is debonding of NSM-FRP bar with surrounding epoxy, and CC is concrete crushing after yielding of steel.

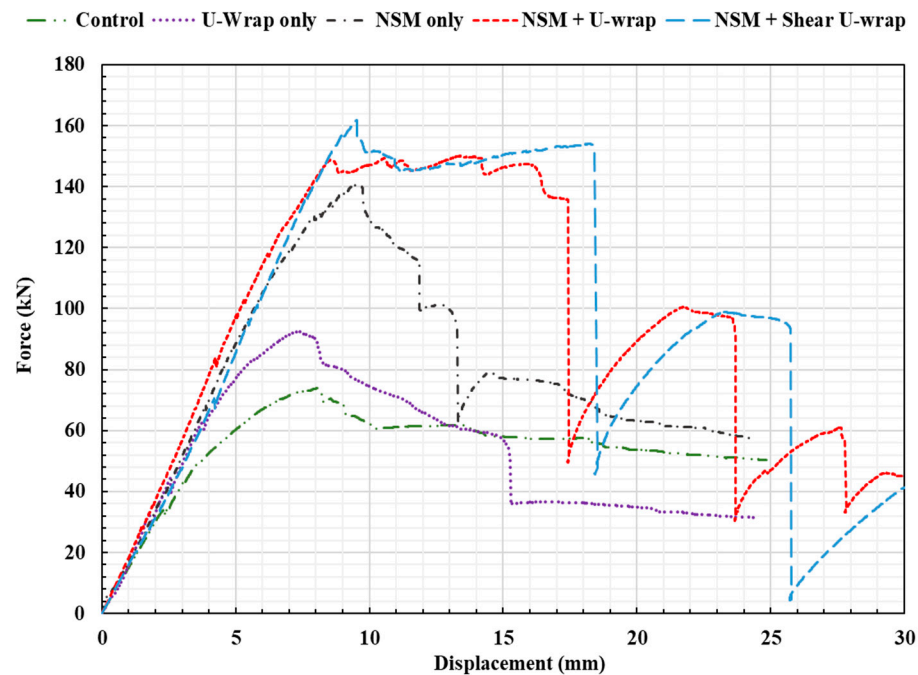


**Figure 12.** Load–displacement behavior of median of all tested beams.

From observation of the load displacement graphs, large load drops are evident after some ductile behavior. Almost all beams had a large load drop of around 18 mm displacement with a load drop rate of 78 kN/mm. There is a noticeable stiffness change between beams, which could be attributed to the change in effect of confinement due to the wrapping or also due to the change in bond developed between the NSM bar and the surrounding epoxy. Beyond the load drop, the beams continued to support the load and observed a decrease in load of more than 50% of the peak. At this point, the test was stopped as the test setup would not allow for any more beam deflection. The “NSU” series beams, incorporating U-wrap in the shear span and NSM-FRP for flexural strengthening, displayed an average ultimate load at failure of 162.17 with a variation of ±6.65 kN. The mean deflection was 14.28 mm, with a standard deviation of 2.23 mm. Their load–deflection pattern was largely akin to that observed in the “NU” series, but in some of the specimens, the failure mode was different. Two of the beams experienced a sudden failure due to the tension rupture of the CFRP. In contrast, the other two showed a progressive failure characterized by continuous CFRP slipping and epoxy splitting until eventual failure occurred. Two of the beams had a large load drop around an 18 mm displacement with a load drop rate of 90 kN/mm. Large drops were not observed in the other two beams where a gradual load decrease was seen. There was a noticeable stiffness change between one of the beams and the rest, which could be attributed to the change in effect of confinement due to the wrapping or also due to the change in bond developed between the NSM bar and the surrounding epoxy.

The data in Figure 13 clearly show that combining U-wrap shear and NSM-FRP flexural strengthening significantly alters beam behavior. It is evident that the control beams have the lowest peak load when compared to the N, U, NU and NSU types. It is evident from this comparison that incorporating NSM flexural strengthening for the control RC beams improves their flexural strength. It can be clearly observed that the NSM-FRP has a significant strength increase in the control specimens as also observed in previous studies [13,17]. The flexural strength is even more dominant because of the high-strength materials, such as the CFRP, which was used to strengthen these beams. Also, it is worth mentioning that the change in slope beyond the linear elastic portion is marginal for N, NU and NSU beam types, which continue in a linear fashion when compared to the C- and U-type beams. This is attributed to the NSM CFRP bar that is highly linear to failure. None of the beams except the combination types (NU and NSU) had significant load drops in the load displacement graphs. Figure 13 provides a summary of these variations in load carrying capacity across the five beam groups. Performing an analysis to compare peak load of control beams to other types of beams, it was observed that there was a 19% increase for U-type beams compared to the control beams. This increase in flexural performance for U-wrap beams can be attributed to the confinement effect. An 83% increase in N-type beams, a 99% increase in NU-type beams and a 105% increase in NSU-type beams was observed, indicating that the incorporation of the CFRP bar as NSM improves flexural strength and even more so in combined beams. This marks a drastic increase in flexural performance in the NSM only and combination-strengthened beams compared to control beams. The combination-strengthened beams were 9% and 12% higher in flexural performance compared to N-type beams, indicating that confining the NSM only beams with the U-wrap improves confinement and bond, thus increasing the flexural strength. In previous work [22], using GFRP NSM, the improvement in flexural performance compared to RC beams was 47%, which is less than the improvement seen in this study as the type of NSM used was CFRP.

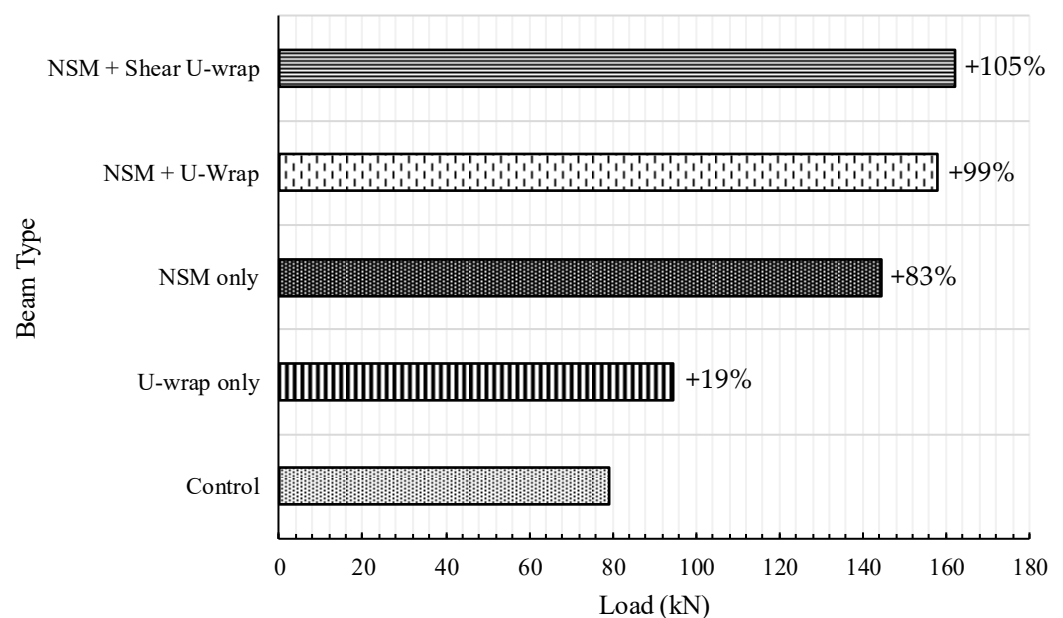


**Figure 13.** Mean flexural load capacity of tested beams. Percentage increase compared to control beams shown on each bar.

Figure 14 illustrates the failure modes for each group of beams. It shows significant debonding in NSM-FRP beams and abrupt CFRP rupture in beams where NSM-FRP is used alongside U-wrap shear reinforcement. The control groups, “C” and “U”, mirrored typical RC beam behavior, failing due to concrete crushing following steel yield. The “N” group experienced CFRP bar and epoxy debonding from the concrete. The “NU” group, showing

improved bond strength, failed due to CFRP bar rupture. The “NSU” group exhibited two failure patterns: either sudden epoxy cover splitting or CFRP bar rupture, depending on the epoxy cover’s efficacy in strain transfer. In cases where the epoxy effectively transferred strain, CFRP bar rupture occurred. Otherwise, the failure was marked by epoxy cover splitting. The CFRP bars in “NU” and “NSU” reached strains up to near their ultimate capacity before failure, indicating that U-wrap confinement helps prevent debonding and allows the bars to achieve higher strain levels. In the experimental findings, it was noted that in the “N” group, the CFRP bar and epoxy started to slip at maximum load due to debonding from the surrounding concrete. Nonetheless, this slippage was not observed in the “NU” group, where CFRP U-wrap was applied along the entire span.

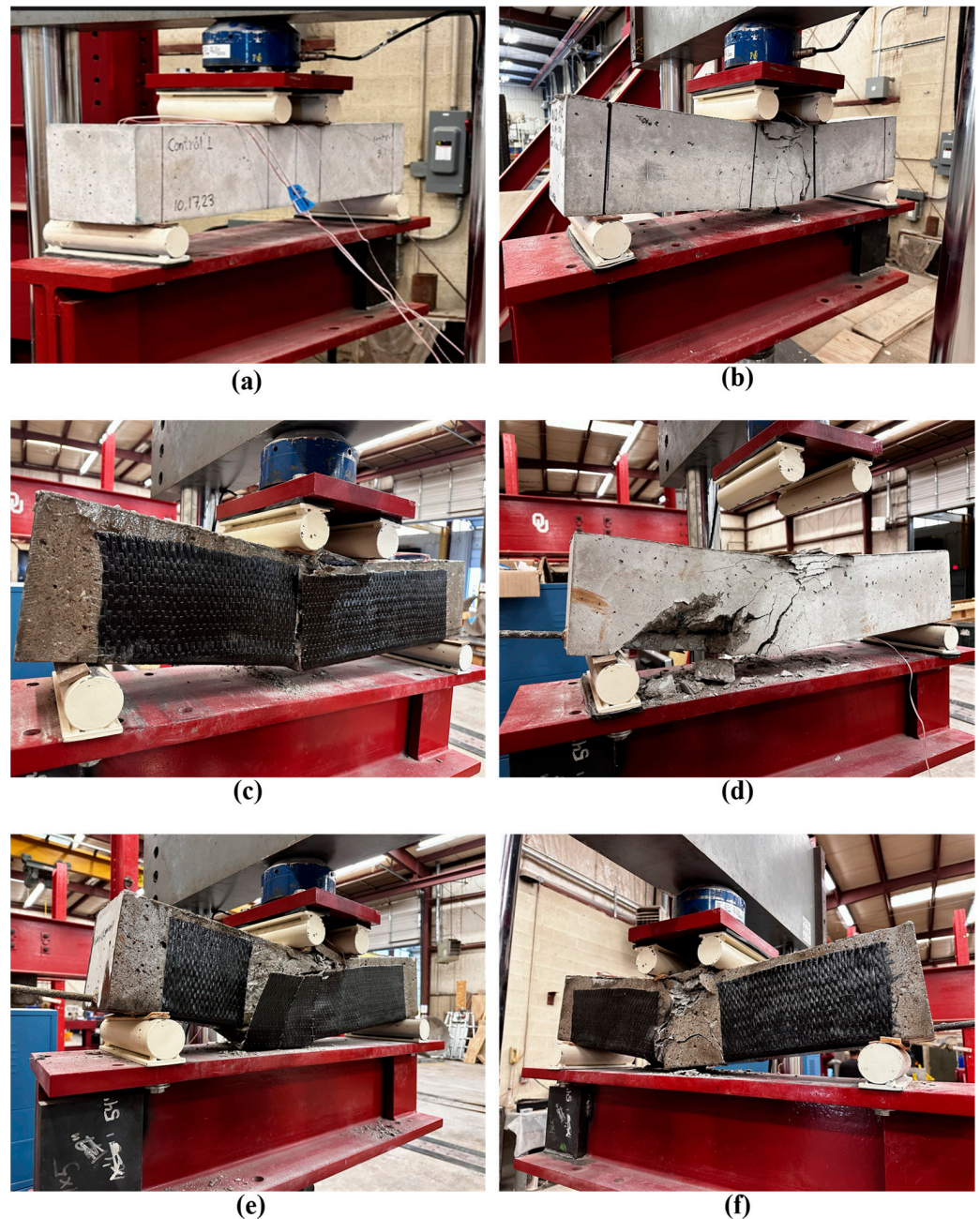


**Figure 14.** Different failure modes of the tested beams. (a) Control beam before performing the test, (b) control beam after performing the test, (c) only U-wrap beam, (d) NSM only beam, (e) NSM + full U-wrap beam, (f) NSM + shear U-wrap beam.

For the “C” control beam group, specifically beam C3, the tension steel reached a yield strain of 0.0021 at a load of 49.3 kN, with a midspan deflection of 4.1 mm. The strain gauge readings ceased at a strain of 0.0052, corresponding to a load of 56.9 kN. Simultaneously, the strain in the top compression fibers of the beam reached 0.003. At this level of strain, the beam experienced failure due to crushing of the concrete. The load at the 0.003 strain level was 74.05 kN, with a midspan deflection of 8.11 mm. In the “N” beam group, for the beam N3, the tension steel reached a strain of 0.0021, while the corresponding CFRP bar strain was 0.0055 at a load of 102.8 kN and a midspan deflection of 5.45 mm. The highest strain recorded in the tension steel was 0.0026 at 149.88 kN load. The CFRP bar’s maximum strain recorded was 0.013 at a load of 153.14 kN, and after that, the beam ultimately failed at a load of 165.51 kN. In the “NU” beam group, specifically at beam NU2, the strain in the tension steel reached 0.0021, with the CFRP bar strain at 0.0025 under a load of 80.94 kN and a midspan deflection of 5.45 mm. The maximum strain in tension steel was 0.004 at a 91.19 kN load. The beam ultimately failed at 150 kN. The failure was abrupt due to CFRP bar rupture, with the bar’s maximum strain reaching 0.0125, which is 70% of the bar’s ultimate tensile strain. In the “NSU” beam group, specifically for NSU4, the tension steel reached a strain of 0.0021, with the CFRP bar strain at 0.0032 under a load of 79.3 kN and a midspan deflection of 5.14 mm. The maximum strain in the tension steel was 0.0044 at a 162.22 kN load, and the beam failed at 163.68 kN. The highest recorded concrete compression strain was 0.00386 at 161.59 kN. Also, the peak strain in the CFRP bar was 0.0119. It is noteworthy that in the “NSU” group of beams, two out of the four experienced failures due to CFRP bar rupture. The strain distribution of type N, NU, and NSU beams is depicted in Figure 15.

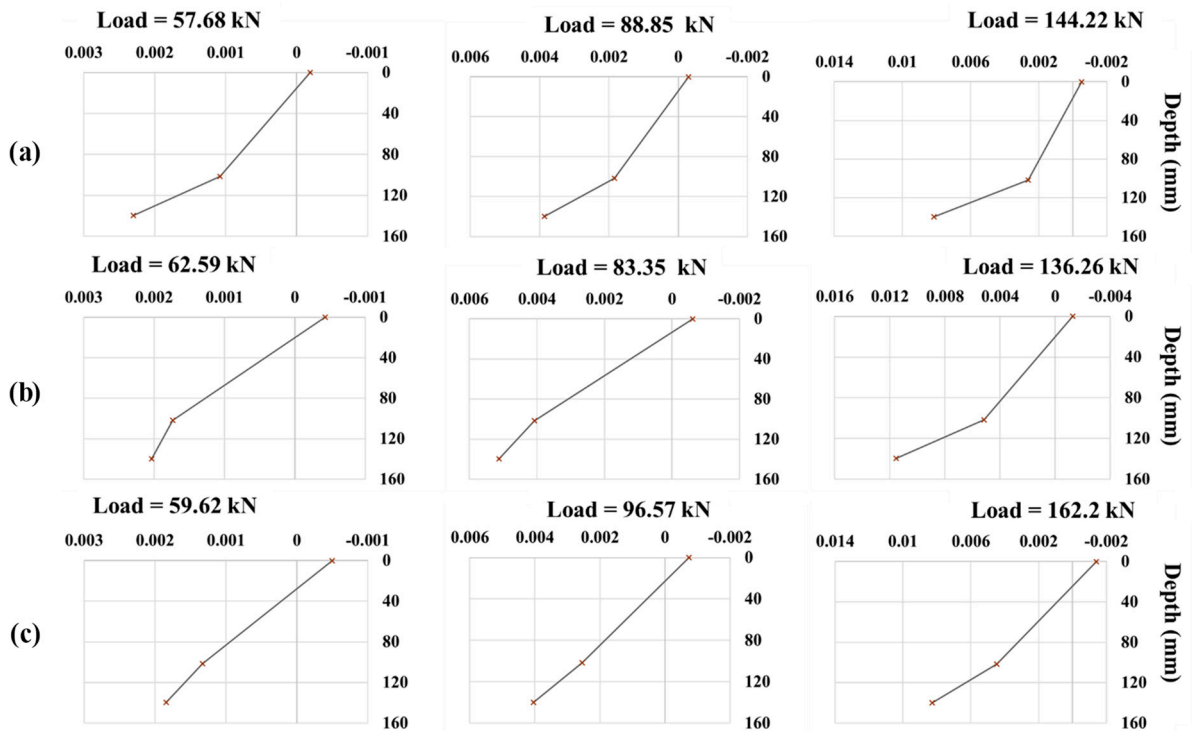


Figure 15. Strain distribution diagrams at various loads for type (a) N, (b) NU, (c) NSU beams.

The failure mode of each beam group is shown in Figure 16. As noted in previous research [17], the integration of NSM-FRP flexural strengthening with U-wrap shear strengthening not only enhances the bonding in RC beams but also maintains their deformability up to the point of failure. This combination effectively improves the overall structural performance without compromising the beam’s ability to deform under load. However, it should be noted that the failure mode for beams strengthened with both U-wrap and

NSM-FRP can be quite sudden and abrupt. This highlights a critical aspect to consider in the combined application of these strengthening techniques. The investigation reveals that combining NSM-FRP and U-wrap shear strengthening in RC beams enhances their load bearing capacity. However, this comes with a trade-off: the strengthened beams are prone to sudden and abrupt failures, along with a rapid loss in capacity, primarily due to the tension rupture of the FRP. As mentioned earlier, 50% of tested NSU beams did not experience sudden failure. So, the investigation interestingly suggests that using U-wrap in the shear span leads to an improved bond in FRP, which effectively enhances the beam's strength. This method manages to increase the bond without the associated risk of sudden failure, a notable benefit in structural engineering applications.



**Figure 16.** Various failure modes of RC beams strengthened with NSM-CFRP, (a) type NU beams, failed by the CFRP bar rupture, (b) type NSU beams, failed by the CFRP bar rupture, (c) type NSU beams, failed by sudden spilling of the epoxy cover.

#### 4. Key Discussion

Based on the strain data of the NSM-CFRP bar, a 33.3% increase was observed for the NU beam series over N beam series showing the improvement in bond between the NSM-FRP bar and surrounding epoxy as a result of U-wraps. However, they were accompanied by bar rupture. U-wrap FRP provides significant external confinement to the concrete, which helps in uniformly distributing the stresses across the concrete section. This confinement effect is particularly beneficial in regions susceptible to high shear stresses and where bending moments induce tensile stresses at the concrete surface. By doing so,

U-wrap effectively delays the initiation and propagation of cracks. From this study, it is evident that special care should be taken in designing RC strengthening combining NSM and U-wrap FRP strengthening.

## 5. Conclusions

In this study, a total of 20 RC beams were organized into five groups. These beams were all subjected to static load testing. The aim of this study was to assess the effects of employing NSM-CFRP for flexural strengthening along with U-wrap CFRP for shear strengthening in concrete structures. This evaluation sought to understand how these methods affect the structural performance concrete beams. Here are some significant conclusions.

1. The obtained results indicated that RC beams reinforced with NSM-FRP exhibited a significant increase in flexural strength, showing an 82% enhancement compared to the control beams. The primary mode of failure observed in these beams was the debonding of the FRP bar and epoxy from the surrounding concrete.
2. The research demonstrated that integrating NSM-FRP for flexural enhancement with full-span U-wrap in RC beams led to an increase in flexural load capacity by approximately 9% compared to beams reinforced only with NSM-FRP. The U-wrap effectively prevented crack growth in the epoxy, improving the bond between NSM-FRP and concrete. This combination altered the failure mode from debonding of the CFRP bar to its rupture at peak tensile strength.
3. The research revealed that applying U-wrap shear strengthening in combination with NSM-FRP flexural strengthening solely in the shear area led to a 12.1% increase in flexural load capacity, compared to beams with NSM-FRP. Among the four beams tested, two failed due to CFRP bar rupture, while the other two experienced sudden epoxy cover splitting. Despite these varying failure modes, strain measurements confirmed that the CFRP bars reached their full tensile capacity, indicating improved bond performance. Both observed failure modes (CFRP rupture and epoxy splitting) were abrupt, impacting the beams' ductility.
4. The integration of U-wrap shear strengthening with NSM-FRP flexural strengthening has shown a marked enhancement in bond performance, increasing the overall flexural load capacity of RC beams. Nevertheless, this combination also led to a shift in failure modes. While NSM-FRP flexural-strengthened beams alone exhibited relatively ductile failure, the addition of full U-wraps, which enhances bond performance through confinement, resulted in more sudden and less ductile failure modes, primarily through bar rupture.
5. The structural design of components is based on a 'fail-safe' concept, necessitating elements to give a warning prior to failure to prevent catastrophes. In infrastructure applications, nonlinear behavior of structural components is important to avoid brittle (catastrophic) failure, which is required by most design codes worldwide. From this study, it is evident that special care should be taken in designing RC strengthening combining NSM and U-wrap FRP strengthening.
6. Future work can be performed with a larger matrix and large-scale beams for further understanding. Positioning LVDTs for the NSM bars can provide information on slippage during testing.

**Author Contributions:** A.A. fabricated and tested specimens, performed analysis of results and contributed towards the paper draft. S.V. curated, supervised the work and contributed towards the paper draft. J.V. supervised the work and contributed towards review of the paper draft. All authors have read and agreed to the published version of the manuscript.

**Funding:** This research was funded by Oklahoma Department of Transportation 2160-23-04 and partially by the University of Oklahoma.

**Data Availability Statement:** The datasets generated during and/or analyzed during the current study are available from the corresponding author on reasonable request.

**Acknowledgments:** The authors would also like to acknowledge the contribution of John Bullock, Royce Floyd, William Jordan and Trent Rogers. The authors would like to thank Rahulreddy Chennareddy for his consulting help.

**Conflicts of Interest:** The contents of this report reflect the views of the author(s) who are responsible for the facts and the accuracy of the data presented herein. The contents do not necessarily reflect the views of the Oklahoma Department of Transportation or the Federal Highway Administration. This report does not constitute a standard, specification, or regulation. While trade names may be used in this report, it is not intended as an endorsement of any machine, contractor, process, or product.

## References

- Gucunski, N.; Pailes, B.; Kim, J.; Azari, H.; Dinh, K. Capture and Quantification of Deterioration Progression in Concrete Bridge Decks through Periodical NDE Surveys. *J. Infrastruct. Syst.* **2017**, *23*, B4016005. [CrossRef]
- Wang, X.; Cheng, L. Bond characteristics and modeling of near-surface mounted CFRP in concrete. *Compos. Struct.* **2021**, *255*, 113011. [CrossRef]
- Sharaky, I.A.; Baena, M.; Barris, C.; Sallam, H.E.M.; Torres, L. Effect of axial stiffness of NSM FRP reinforcement and concrete cover confinement on flexural behaviour of strengthened RC beams: Experimental and numerical study. *Eng. Struct.* **2018**, *173*, 987–1001. [CrossRef]
- Vedernikov, A.; Tucci, F.; Carlone, P.; Gusev, S.; Konev, S.; Firsov, D.; Akhatov, I.; Safonov, A. Effects of pulling speed on structural performance of L-shaped pultruded profiles. *Compos. Struct.* **2021**, *255*, 112967. [CrossRef]
- Bakis, C.E.; Bank, L.C.; Brown, V.L.; Cosenza, E.; Davalos, J.F.; Lesko, J.J.; Machida, A.; Rizkalla, S.H.; Triantafyllou, T.C. Fiber-Reinforced Polymer Composites for Construction—State-of-the-Art Review. *Perspect. Civ. Eng. Commem. 150th Anniv. Am. Soc. Civ. Eng.* **2003**, *6*, 369–383. [CrossRef]
- Van Den Einde, L.; Zhao, L.; Seible, F. Use of FRP composites in civil structural applications. *Constr. Build. Mater.* **2003**, *17*, 389–403. [CrossRef]
- Tharmarajah, G.; Taylor, S.E.; Cleland, D.J.; Robinson, D. Corrosion-resistant FRP reinforcement for bridge deck slabs. *Proc. Inst. Civ. Eng.-Bridg. Eng.* **2015**, *168*, 208–217. [CrossRef]
- Liu, X.; Nanni, A.; Silva, P.F. Rehabilitation of compression steel members using FRP pipes filled with non-expansive and expansive light-weight concrete. *Adv. Struct. Eng.* **2005**, *8*, 129–141. [CrossRef]
- Bizindaviyi, L.; Neale, K.W.; Erki, M.A. Experimental Investigation of Bonded Fiber Reinforced Polymer-Concrete Joints under Cyclic Loading. *J. Compos. Constr.* **2003**, *7*, 127–134. [CrossRef]
- Sokairge, H.; Elgabbas, F.; Elshafie, H. Structural behavior of RC beams strengthened with prestressed near surface mounted technique using basalt FRP bars. *Eng. Struct.* **2022**, *250*, 113489. [CrossRef]
- Kadhim, M.M.A.; Jawdhari, A.; Altaee, M.M.; Majdi, A.; Fam, A. Parametric investigation of continuous beams strengthened with near surface mounted FRP bars. *Eng. Struct.* **2023**, *293*, 116619. [CrossRef]
- Kabashi, N.; Avdyli, B.; Krasniqi, E.; Këpuska, A. Comparative approach to flexural behavior of reinforced beams with GFRP, CFRP, and steel bars. *Civ. Eng. J.* **2020**, *6*, 50–59. [CrossRef]
- Sbahieh, S.; McKay, G.; Al-Ghamdi, S.G. A comparative life cycle assessment of fiber-reinforced polymers as a sustainable reinforcement option in concrete beams. *Front. Built Environ.* **2023**, *9*, 1194121. [CrossRef]
- Zhang, S.S.; Yu, T.; Chen, G.M. Reinforced concrete beams strengthened in flexure with near-surface mounted (NSM) CFRP strips: Current status and research needs. *Compos. Part B Eng.* **2017**, *131*, 30–42. [CrossRef]
- Guide for the Design and Construction of Externally Bonded FRP Systems for Strengthening Concrete Structures. 2017. Available online: [www.concrete.org](http://www.concrete.org) (accessed on 6 February 2024).
- Saadatmanesh, H.; Ehsani, M.R. Fiber composite plates can strengthen beams. *Concr. Int.* **1990**, *12*, 65–71. Available online: <https://www.concrete.org/publications/internationalconcreteabstractportal/m/details/id/2060> (accessed on 29 December 2023).
- Nanni, A.; Alkhrdaji, T.; Chen, G.; Barker, M.; Xinbao, Y.; Mayo, R. Overview of testing to failure program of a highway bridge strengthened with FRP composites. In Proceedings of the 4th International Symposium on FRP for Reinforcement of Concrete Structures (FRPRCS4), Baltimore, MD, USA; 1999; pp. 69–80. Available online: [https://www.researchgate.net/profile/Antonio-Nanni-3/publication/241138044\\_OVERVIEW\\_OF\\_TESTING\\_TO\\_FAILURE\\_PROGRAM\\_OF\\_A\\_HIGHWAY\\_BRIDGE\\_STRENGTHENED\\_WITH\\_FRP\\_COMPOSITES/links/004635321cdb15c37300000/OVERVIEW-OF-TESTING-TO-FAILURE-PROGRAM-OF-A-HIGHWAY-BRIDG](https://www.researchgate.net/profile/Antonio-Nanni-3/publication/241138044_OVERVIEW_OF_TESTING_TO_FAILURE_PROGRAM_OF_A_HIGHWAY_BRIDGE_STRENGTHENED_WITH_FRP_COMPOSITES/links/004635321cdb15c37300000/OVERVIEW-OF-TESTING-TO-FAILURE-PROGRAM-OF-A-HIGHWAY-BRIDG) (accessed on 29 December 2023).
- De Lorenzis, L.; Teng, J.G. Near-surface mounted FRP reinforcement: An emerging technique for strengthening structures. *Compos. Part B Eng.* **2007**, *38*, 119–143. [CrossRef]
- Van Cao, V.; Pham, S.Q. Comparison of CFRP and GFRP Wraps on Reducing Seismic Damage of Deficient Reinforced Concrete Structures. *Int. J. Civ. Eng.* **2019**, *17*, 1667–1681. [CrossRef]
- Zhang, S.S.; Teng, J.G.; Yu, T. Bond Strength Model for CFRP Strips Near-Surface Mounted to Concrete. *J. Compos. Constr.* **2014**, *18*, A4014003. [CrossRef]
- Chennareddy, R.; Taha, M.M.R. Effect of Combining Near-Surface-Mounted and U-Wrap Fiber-Reinforced Polymer Strengthening Techniques on Behavior of Reinforced Concrete Beams. *ACI Struct. J.* **2017**, *114*, 721–730. [CrossRef]

22. ChennaReddy, R. Significance of U-Wrap FRP Shear Strengthening on Flexural Behavior of RC Beams Strengthened Using Near Surface Mounted FRP Bars (700 mm Beam). 2016. Available online: <http://search.ebscohost.com/login.aspx?direct=true&db=ddu&AN=EC93B2989CA19E9C&site=ehost-live> (accessed on 1 February 2016).
23. Murad, Y.; Abu-AlHaj, T. Flexural strengthening and repairing of heat damaged RC beams using continuous near-surface mounted CFRP ropes. *Structures* **2021**, *33*, 451–462. [[CrossRef](#)]
24. Kachlakev, D.; McCurry, D.D. Behavior of full-scale reinforced concrete beams retrofitted for shear and flexural with FRP laminates. *Compos. Part B Eng.* **2000**, *31*, 445–452. [[CrossRef](#)]
25. Chajes, M.J.; Januszka, T.F.; Mertz, D.R.; Thomson, T.A.; Finch, W.W. Shear strengthening of reinforced concrete beams using externally applied composite fabrics. *ACI Struct. J.* **1995**, *92*, 295–303. [[CrossRef](#)] [[PubMed](#)]
26. Taerwe, L. Rehabilitation of navy pier beams with composite sheets. In *Non-Metallic (FRP) Reinforcement for Concrete Structures*; Chapman & Hall: London, UK, 2020; pp. 551–558. [[CrossRef](#)]
27. Ombres, L.; Mazzuca, P. Residual Flexural Behavior of PBO FRCM-Strengthened Reinforced Concrete Beams after Exposure to Elevated Temperatures. *J. Compos. Constr.* **2024**, *28*, 04023063. [[CrossRef](#)]
28. Wuertz, A.F. Strengthening Rectangular Beams with NSM Steel Bars and Externally Bonded GFRP. 2013. Available online: <https://krex.k-state.edu/bitstream/handle/2097/15624/AugustineWuertz2013.pdf?sequence=3> (accessed on 9 January 2024).
29. *ASTM/C143M-15a*; Standard Test Method for Slump of Hydraulic Cement Concrete (C 143). ASTM International: West Conshohocken, PA, USA, 2009; Volume 27, pp. 99–101. Available online: [https://www.astm.org/c0143\\_c0143m-00.html](https://www.astm.org/c0143_c0143m-00.html) (accessed on 5 February 2022).
30. *ASTM C39*; Standard Test Method for Compressive Strength of Cylindrical Concrete Specimens. ASTM International: West Conshohocken, PA, USA, 2001.
31. *ASTM C496-96*; Standard Test Method for Splitting Tensile Strength of Cylindrical Concrete Specimens. Annual Book of ASTM Standards: West Conshohocken, PA, USA, 2022; Volume i, pp. 1–5. [[CrossRef](#)]
32. *ASTM C469/C469M-14*; Standard Test Method for Static Modulus of Elasticity and Poisson’s Ratio of Concrete in Compression. Annual Book of ASTM Standards: West Conshohocken, PA, USA, 2014; pp. 1–5. [[CrossRef](#)]

**Disclaimer/Publisher’s Note:** The statements, opinions and data contained in all publications are solely those of the individual author(s) and contributor(s) and not of MDPI and/or the editor(s). MDPI and/or the editor(s) disclaim responsibility for any injury to people or property resulting from any ideas, methods, instructions or products referred to in the content.